

SPECTROSCOPIC REDSHIFTS TO $Z > 2$ FOR OPTICALLY OBSCURED SOURCES DISCOVERED WITH THE SPITZER SPACE TELESCOPE

J. R. HOUCK¹, B. T. SOIFER², D. WEEDMAN¹, S. J. U. HIGDON¹, J. L. HIGDON¹, T. HERTER¹, M. J. I. BROWN^{3,4}, A. DEY⁴, B. T. JANNUZI⁴, E. LE FLOC'H⁵, M. RIEKE⁵, L. ARMUS², V. CHARMANDARIS¹, B. R. BRANDL⁷, & H. I. TEPLITZ²

Draft version September 19, 2018

ABSTRACT

We have surveyed a field covering 9.0 degrees² within the NOAO Deep Wide-Field Survey region in Boötes with the Multiband Imaging Photometer on the Spitzer Space Telescope (SST) to a limiting 24 μm flux density of 0.3 mJy. Thirty one sources from this survey with $F_{24\mu\text{m}} > 0.75$ mJy which are optically very faint ($R \gtrsim 24.5$ mag) have been observed with the low-resolution modules of the Infrared Spectrograph on SST. Redshifts derived primarily from strong silicate absorption features are reported here for 17 of these sources; 10 of these are optically invisible ($R \gtrsim 26$ mag), with no counterpart in B_W , R , or I . The observed redshifts for 16 sources are $1.7 < z < 2.8$. These represent a newly discovered population of highly obscured sources at high redshift with extreme infrared to optical ratios. Using IRS spectra of local galaxies as templates, we find that a majority of the sources have mid-infrared spectral shapes most similar to ultraluminous infrared galaxies powered primarily by AGN. Assuming the same templates also apply at longer wavelengths, bolometric luminosities exceed $10^{13}L_{\odot}$.

Subject headings: dust, extinction — galaxies: high-redshift – infrared: galaxies — galaxies: starburst
galaxies: AGN

1. INTRODUCTION

Opening the infrared wavelength regime for discovery is a primary objective of the final Great Observatory, the Spitzer Space Telescope (Werner et al. 2004). It was anticipated that new categories of sources would be revealed in various surveys. It was also anticipated that some of these sources would be very faint optically, as dust obscuration is probable in infrared-luminous sources, so the Infrared Spectrograph on Spitzer (IRS⁷ – Houck, et al. 2004) was designed to include low resolution modules which could determine redshifts for dusty sources. High-redshift, optically faint but infrared-loud galaxies were first hinted at by the deepest IRAS surveys (Houck et al. 1984), and partially uncovered in deep surveys with ISO (Dole et al. 2001, Elbaz et al. 2002). The sensitivity and wavelength coverage of the IRS enables us to measure the redshifts and power sources within such galaxies even if they are too faint for optical spectroscopy.

In order to search for such optically-faint infrared sources, we have surveyed the Boötes field of the NOAO Deep Wide-Field Survey (NDWFS, Jannuzi & Dey (1999)) with the Multiband Imaging Photometer for Spitzer (MIPS; Rieke et al. (2004)) to produce a catalog of mid-infrared sources in 9.0 deg² to flux density limits at 24 μm of 0.3 mJy. This field was chosen because the deep and well calibrated optical imagery in B_W , R ,

and I bands makes possible the identification of infrared sources with very faint optical counterparts and confident selection of infrared sources lacking optical counterparts to very deep limits. Our overall objective for the current study was to select the infrared sources which are faintest optically but bright enough for feasible redshift determination with the IRS, taking a limit of 0.75 mJy for these initial observations.

Details of the survey will be reported elsewhere. We used the MIPS and optical surveys to select and inspect all sources with 24 μm flux densities above 0.75 mJy and with $I \geq 24$ mag. Of the 4273 MIPS 24 μm sources brighter than 0.75 mJy, 114 met this optical magnitude criterion. Of these, 27 sources have no optical identification in any band, meaning they are fainter than about 26.5 mag in B_W , 26 mag in R , and 25.5 mag in I (all Vega magnitudes). Based on comparison of positions between the many identified optical counterparts and infrared sources, the formal 5σ positional criterion for non-identification of 24 μm sources with flux densities above 0.75 mJy is a distance $> 2''$ from the nearest optical source. We also rejected infrared sources close to a bright galaxy or within clusters of faint galaxies with the presumption that redshifts of the infrared sources can be determined by association with the optical sources. As a result of these additional criteria, our initial target list contained 17 sources with no optical identifications, and all of these have been observed with the IRS. We also observed an additional 13 sources having an optical counterpart but fainter than 24.5 mag in R . Finally, one source was included (#13 in Table 1) because it is relatively bright at 24 μm but has an extreme IR/optical ratio (2.3 mJy at 24 μm and $R=23.8$ mag). In this paper, we report redshifts, physical properties and luminosities for 17 of the 31 sources which show sufficiently strong spectral features that redshift measurements can be made with the IRS.

¹ Astronomy Department, Cornell University, Ithaca, NY 14853; jrh13@astro.cornell.edu

² Spitzer Science Center, California Institute of Technology, 220-6, Pasadena, CA 91125

³ Department of Astrophysical Sciences, Princeton University, Peyton Hall, Princeton, NJ 08544-1001

⁴ National Optical Astronomy Observatory, Tucson, AZ 85726

⁵ Steward Observatory, University of Arizona, Tucson, AZ 85721

⁶ Leiden Observatory, 2300 RA Leiden, The Netherlands

⁷ The IRS was a collaborative venture between Cornell University and Ball Aerospace Corporation funded by NASA through the Jet Propulsion Laboratory and the Ames Research Center

2. OBSERVATIONS AND DATA REDUCTION

Observations and results for the sources discussed in this paper are summarized in Table 1, giving the name (with full coordinates), the $24\ \mu\text{m}$ flux density, optical magnitudes of the MIPS $24\ \mu\text{m}$ source if detected, integration times for the IRS observations, redshift determinations, and other source characteristics. The MIPS data were obtained with an effective integration time of ~ 90 sec per sky pixel and reduced with the MIPS Data Analysis Tool (Gordon et al. 2004). Point source extraction was performed using an empirical point spread function (PSF) constructed from the brightest objects found in the $24\ \mu\text{m}$ image and subsequently fitted to all the sources detected in the data. We allowed for a multiple match fitting to deal with blended cases. We finally derived the flux of each object using the scaled fitted PSF after applying a slight correction to account for the finite size of the modeled point spread function.

Spectroscopic observations were made with the IRS Short Low module in order 1 only (SL1) and with the Long Low module in orders 1 and 2 (LL1 and LL2), described in Houck et al. (2004). These give low resolution spectral coverage from $\sim 8\ \mu\text{m}$ to $\sim 35\ \mu\text{m}$. Sources were placed on the slits by offsetting from nearby 2MASS stars. Observed images were processed with version 10.5 of the SSC pipeline. Background subtraction and extraction of source spectra along the slit was done with the SMART analysis package (Higdon et al. 2004b). All spectra discussed in this paper are shown in Figures 1 and 2.

3. DETERMINING REDSHIFTS OF SOURCES

We determine redshifts by using bright, local “template” sources for which we have full spectral coverage with the IRS. In almost all cases, a redshift fit depends on the presence of a strong decrease in the continuous spectrum beginning around $9\ \mu\text{m}$ in the source rest frame (for example, see Higdon et al. (2004a)). This drop is identified with the strong silicate absorption feature centered at $9.7\ \mu\text{m}$; this feature is common in ultraluminous infrared galaxies (ULIRGs) at low redshift (e.g. Armus et al. 2004). An extreme case of this type of absorption is seen in the IRS spectrum of the ULIRG IRAS F00183-7111 (Spoon et al. 2004a). Strong spectral emission features, such as the $7.7\ \mu\text{m}$ and $8.6\ \mu\text{m}$ PAH features, can be present without the presence of deep silicate absorption – e.g., in the unobscured starburst nucleus of NGC 7714 (Brandl et al. 2004). The well known low-redshift ULIRGs Arp 220 and Mrk 231 are intermediate cases. Arp 220 has deep silicate absorption and strong PAH emission (Spoon et al. 2004b), while Mrk 231 has weak silicate absorption, but little or no PAH emission. To cover the range from pure absorption to pure emission, we have fit all spectra with the IRS templates of NGC 7714, F00183-7111, Arp 220, and Mrk 231. (The IRS spectra of Arp 220 and Mrk 231 will be discussed in more detail in future papers.) A formal χ^2 routine gives the optimal redshift fit for each template. Once such fits were formally determined, the four were compared to estimate which one gave overall the best fit to the observed spectrum. That is the result listed in Table 1 and shown in Figure 1.

Figure 2 illustrates the effects of alternative templates for our brightest $24\ \mu\text{m}$ source, #9 in Table 1, showing

that the redshift uncertainty for a given source primarily depends on source S/N and strength of the features rather than choice of template. For the sources in Table 1, this uncertainty typically is ± 0.2 in z ; the formal uncertainty derived from the χ^2 fit for the template adopted is given for each source in Table 1.

The 17 sources out of our 31 observed spectra with measured redshifts derived from template fits are all shown in Figure 1. The 14 remaining sources do not have sufficiently strong features to list a spectroscopic redshift. An example of one of these sources is also shown in Figure 1 to illustrate the obvious difference between spectra with and without strong mid-infrared features. Of the 17 sources, 15 have unambiguous redshifts based on the χ^2 fits shown, and all of these have $1.7 < z < 2.8$. The two sources for which we have less confidence in the redshift include the only source, #11, with assigned $z < 1$. The redshift of 0.70 arises because all three of the templates containing absorption give a better fit at this redshift than at the higher redshifts characterizing all of the other sources; however, the spectrum beyond $30\ \mu\text{m}$ for this source does not have sufficient S/N to show the drop in flux density which would be present for a strong absorption feature at high redshift. Source #2 is the only source for which the template fits produce an ambiguous redshift based on χ^2 . Comparably good fits arise from Arp 220 at $z = 0.57$ or NGC 7714 at $z = 1.86$. The NGC 7714 fit is adopted because of our presumption that a dusty source is more likely to be optically faint at high redshift, but if this fit is correct, this is the only source with a pure PAH emission spectrum.

4. DISCUSSION

These results clearly demonstrate the presence of a population of optically-obscured infrared sources at redshifts $1.7 < z < 2.8$. There are significant selection effects in our result that constrain the redshift range in which we can identify this obscured population. We have deliberately selected against optically visible sources, which generally forces sources to significant redshift, probably $z \gtrsim 1$, because the rest-frame UV is most affected by internal obscuration. For $1.0 \lesssim z \lesssim 1.6$, any deep $9.7\ \mu\text{m}$ silicate absorption feature in the spectrum would significantly affect survey detections at $24\ \mu\text{m}$, so absorbed objects would selectively fall out of the $24\ \mu\text{m}$ sample. For $z \gtrsim 3.1$, the continuum drop indicating the absorption feature would move out of the IRS spectral coverage. It is not surprising, therefore, that the redshifts we have identified fall in the range $1.6 < z < 3.1$. Within this range, our initial results represent only a lower limit for the extent of this obscured population. This is primarily because of our restriction to sources brighter than $0.75\ \text{mJy}$ at $24\ \mu\text{m}$, but also because many sufficiently bright infrared sources with faint optical counterparts (the 84 remaining sources having an optical identification but with $I > 24\ \text{mag}$) were excluded from IRS observation in the hope that redshifts for these very faint sources might be determinable with ground-based spectroscopy.

Even though the sources in our sample are faint, their high redshifts require luminosities that place them among the class of extreme or “hyper-luminous” infrared galaxies. However, these sources have been chosen because they are extremely faint in the optical, implying much larger intrinsic extinction than in a typical

ULIRG. For example, an object having the infrared SED of Arp 220 and sufficiently luminous to have a $24\ \mu\text{m}$ flux density of 1 mJy when at $z = 2$ would have $I < 23$ mag, making it too bright in the optical to be included in our sample. (A source of the same luminosity as Arp 220 if at $z = 2$ would be much too faint to be included in our infrared sample, having a $24\ \mu\text{m}$ observed flux density of only 0.03 mJy.) Thus, while our sources have IRS spectra that can be well fit with known ULIRG templates in the rest-frame mid-infrared, they are all much fainter optically, and therefore apparently more heavily extinguished, than low-redshift ULIRGs. What is the nature of this obscured population? Is the mid-infrared luminosity of the hot dust produced primarily by an AGN or by a starburst in our sample galaxies? If IRAS F00183-7111 is powered by an AGN, as suggested by Spoon et al. (2004b), then 13 out of 17 (76%) of the sample are best fit with an AGN mid-IR template (F00183-7111 or Mrk 231). Four of the galaxies are best fit with a starburst template (Arp 220 or NGC 7714). Although the fraction of light coming from an AGN or from a starburst in any ULIRG is uncertain, these template fits suggest that most of the sources we have found are AGN dominated – i.e. steeply rising spectra with weak PAH emission features and varying levels of silicate absorption.

Radio data can also aid in understanding the nature of these sources. A well defined correlation exists between infrared and radio flux densities for systems with no AGN contribution to the radio flux density. Appleton et al. (2004) show that this relation as described by the parameter $q = \log[f_\nu(24\ \mu\text{m})/f_\nu(20\ \text{cm})]$ has $q = 0.8 \pm 0.3$. The Boötes survey area has been mapped as part of a Westerbork 20 cm survey (de Vries et al. 2002). Although the radio beam ($13'' \times 27''$) is much larger than even the MIPS $24\ \mu\text{m}$ beam, we attempt source identifications by considering any $24\ \mu\text{m}$ source that has a quoted Westerbork source within $5''$ to be an identification with this radio source. With this criterion, five of the infrared sources have radio counterparts. For those that do not, we take the upper limit to the 20 cm flux density to be a 5σ value of 0.20 mJy. The q values are listed in Table 1. Except for source #13, all sources have values or limits for q very close to those expected for starbursts or radio-quiet AGN. Source #13 does have the excess radio emission which would characterize a radio-loud AGN, and this source is best fit with the IRAS F00183-7111 template, confirming at least for this case the validity of the AGN interpretation.

To understand the contribution of this obscured population to the luminosity density of the universe at high redshift, estimates of bolometric luminosities are needed. Our only way to estimate these is to assume that mid-infrared luminosities scale to bolometric luminosities the same as in the template sources which fit the mid-infrared spectra. Using this scaling, all sources in Table 1 for which we have $z > 1.7$ have implied infrared luminosities of $6 \times 10^{12} - 6 \times 10^{13} L_\odot$, with an average value of $2.3 \times 10^{13} L_\odot$. The largest existing samples of dusty sources with comparable bolometric luminosities and redshifts are the SCUBA or MAMBO submillimeter-selected galaxies (Chapman et al. 2003). Detection at

$24\ \mu\text{m}$ of such sources brighter than a few mJy at submillimeter wavelengths is common, but nearly all of these galaxies are fainter at $24\ \mu\text{m}$ by a typical factor of 3–5 than the sources reported here (e.g. Ivison et al. (2004), Egami et al. (2004), Frayer et al. (2004), and Charmandaris et al. (2004)). This implies a higher ratio of mid-infrared to far-infrared luminosity in our sources than in the sub-millimeter sources. This indicates that our new sample seems to represent sources that have hotter dust than typical submillimeter-selected galaxies; this could be an additional component of hot dust or an overall averaged dust temperature which is greater. Either would be consistent with having AGN as the primary luminosity source instead of the starbursts thought to power the sub-millimeter galaxies. Chapman et al. (2004) utilized optically determined redshifts to identify a population of optically faint radio galaxies ($R > 23.5$ mag) at $z \sim 2$ which are not detected as submillimeter sources, and half of this sample has optical indicators of an AGN. Although none of the sources were observed in the infrared, Chapman et al. (2004) suggest from the absence of submillimeter detections that this sample is also characterized by hot dust, so it may represent a similar population to our sample.

5. SUMMARY

The NOAO Deep Wide-Field Survey area in Boötes has been surveyed at $24\ \mu\text{m}$ with the MIPS instrument on SST, and 31 optically faint or invisible sources have been observed with the IRS instrument. Our first results indicate that sources chosen solely on the basis of extreme $24\ \mu\text{m}$ to I band flux density ratios, $\nu f_\nu(24\ \mu\text{m})/\nu f_\nu(I) \gtrsim 100$, are heavily selected in favor of redshifts exceeding 1.5 and that the majority of such sources have redshifts that are measurable with IRS based on a strong silicate absorption feature in the mid-infrared. Sixteen of the 31 objects selected for the initial IRS observations are found to have spectroscopic redshifts $1.7 < z < 2.8$, based on fits of redshifted IRS spectral templates for local ULIRGS, and 9 of these have no optical counterparts. The template spectra and radio survey data suggest that this population is dominated by AGN-powered, radio-quiet ULIRGs. If bolometric luminosities scale with mid-infrared luminosities as in the templates, these newly discovered sources have bolometric luminosities between $6 \times 10^{12} L_\odot$ and $6 \times 10^{13} L_\odot$.

We thank many others on the IRS, MIPS, and Boötes Survey teams for contributing to this effort, especially including D. Barry, D. Devost, P. Hall, G. Sloan, H. Dole, P. Appleton, and C. Bian. This work is based in part on observations made with the Spitzer Space Telescope, which is operated by the Jet Propulsion Laboratory, California Institute of Technology under NASA contract 1407. Support for this work was provided by NASA through Contract Number 1257184 issued by JPL/Caltech. This work used data provided by the NDWFS, which is supported by NOAO. NOAO is operated by AURA, Inc., under an agreement with the NSF.

REFERENCES

- Brandl, B. R., et al. 2004, ApJS, 154, 188
Chapman, S.C., Blain, A.W., Ivison, R.J. and Smail, I.R. 2003, Nature, 422, 695
Chapman, S.C., Smail, I., Blain, A.W. and Ivison, R.J., 2004, ApJ, 616, 71
Charmandaris, V. et al. 2004, ApJS, 154, 142 i
de Vries, W.H. et al. 2002, AJ, 123, 1784
Dole, H., et al. 2001, A&A, 372, 364
Egami, E. et al. 2004, ApJS, 154, 130
Elbaz, D., Cesarsky, C. J., Chanical, P., Aussel, H., Franceschini, A., Fadda, D., & Chary, R. R. 2002, A&A, 384, 848
Frayser, D.T. et al. 2004, ApJS, 154, 137
Gordon, K., et al., 2004, PASP, submitted
Higdon, S. J. U., et al 2004, ApJS, 154, 174
Higdon, S. J. U., et al 2004, PASP, 116, 975
Houck, J. R., et al. 1984, ApJ, 278, L63
Houck, J. R., et al. 2004, ApJS, 154, 18
Ivison, R.J. et al. 2004, ApJS, 154, 124
Jannuzi, B. T. & Dey, A., 1999, in "Photometric Redshifts and the Detection of High Redshift Galaxies", ASP Conference Series, Vol. 191, Edited by R. Weymann, L. Storrie-Lombardi, M. Sawicki, and R. Brunner. ISBN: 158381-017-X, p. 111
Rieke, G. H., et al. 2004 ApJS154, 24
Spoon, H. W. W., et al. 2004, ApJS, 154, 184
Spoon, H. W. W., Moorwood, A. F. M., Lutz, D., Tielens, A. G. G. M., Siebenmorgen, R., & Keane, J. V. 2004, A&A, 414, 873
Werner, M. W., et al. 2004, ApJS, 154, 1

TABLE 1
 REDSHIFTS AND SOURCE CHARACTERISTICS

Source	Name ^a	f_{ν} 24 μ m (mJy)	B_W (mag)	R (mag)	I (mag)	time ^b (sec)	z	Template	IR/opt ^c	q	L_{ir} ^d ($\times 10^{13} L_{\odot}$)
1.	SST24 J142958.33+322615.4	1.24	25.6	25.1	24.4	1200	2.64 \pm .25	F00183-7111	110	>0.8	1.8
2.	SST24 J142653.23+330220.7	0.89	24.7	1680	1.86 \pm .07	NGC 7714	100	>0.8	0.9
3.	SST24 J143447.70+330230.6	1.81	960	1.78 \pm .30	Mrk 231	>270	0.8	0.9
4.	SST24 J143523.99+330706.8	1.08	26.7	24.6	23.5	1440	2.59 \pm .34	F00183-7111	40	0.8	1.5
5.	SST24 J142804.12+332135.2	0.87	1680	2.34 \pm .28	F00183-7111	>130	>0.6	0.9
6.	SST24 J143358.00+332607.1	1.03	1440	1.96 \pm .34	Mrk 231	>150	>0.7	0.6
7.	SST24 J143251.82+333536.3	0.78	26.2	...	24.3	1920	1.78 \pm .14	Arp 220	60	>0.8	2.8
8.	SST24 J143539.34+334159.1	2.65	26.2	25.4	24.5	720	2.62 \pm .26	F00183-7111	250	>1.1	3.8
9.	SST24 J143001.91+334538.4	3.83	480	2.46 \pm .20	F00183-7111	>570	1.0	4.6
10.	SST24 J143520.75+340418.2	1.45	25.5	25.3	24.3	1200	2.08 \pm .21	Mrk 231	110	>0.8	1.0
11.	SST24 J143242.51+342232.1	0.87	1680	0.70 \pm .24	Mrk 231	>130	>0.6	3.0
12.	SST24 J142626.49+344731.2	1.12	1440	2.13 \pm .09	Arp 220	>170	0.8	5.7
13.	SST24 J143644.22+350627.4	2.30	24.7	23.7	23.4	720	1.95 \pm .17	F00183-7111	80	-0.3	1.8
14.	SST24 J142538.22+351855.2	0.79	1920	2.26 \pm .11	Arp 220	>120	>0.6	5.3
15.	SST24 J142645.71+351901.4	1.05	1440	1.75 \pm .21	Mrk 231	>160	>0.8	0.5
16.	SST24 J142924.83+353320.3	1.04	1440	2.73 \pm .19	F00183-7111	>150	>0.7	1.6
17.	SST24 J143504.12+354743.2	1.23	1200	2.13 \pm .17	Mrk 231	>180	>0.8	0.9

^aSST24 source name derives from discovery with the MIPS 24 μ m images; coordinates listed are J2000 24 μ m positions with typical 3σ uncertainty of $\pm 1.2''$; sources with an optical counterpart will also appear in NDWFS catalogs with prefix NDWFS and the optical source position; optical magnitudes are Mag-Auto from NDWFS Data Release Three, available at <http://www.noao.edu/noao/noaodeep/>.

^bIntegration time for each order of Long Low spectrum; integration time in Short Low order 1 is 480 s in all cases.

^cIR/opt = $\nu f_{\nu}(24\ \mu\text{m})/\nu f_{\nu}(I)$. Limits are based on assumed $I > 25$.

^dThe intrinsic infrared luminosity of each source, $L_{ir} = L(8\text{-}1000\ \mu\text{m})$, is estimated by scaling the known L_{ir} of the best template fit to the measured MIPS 24 μ m flux density after redshifting the template SED to its measured z .

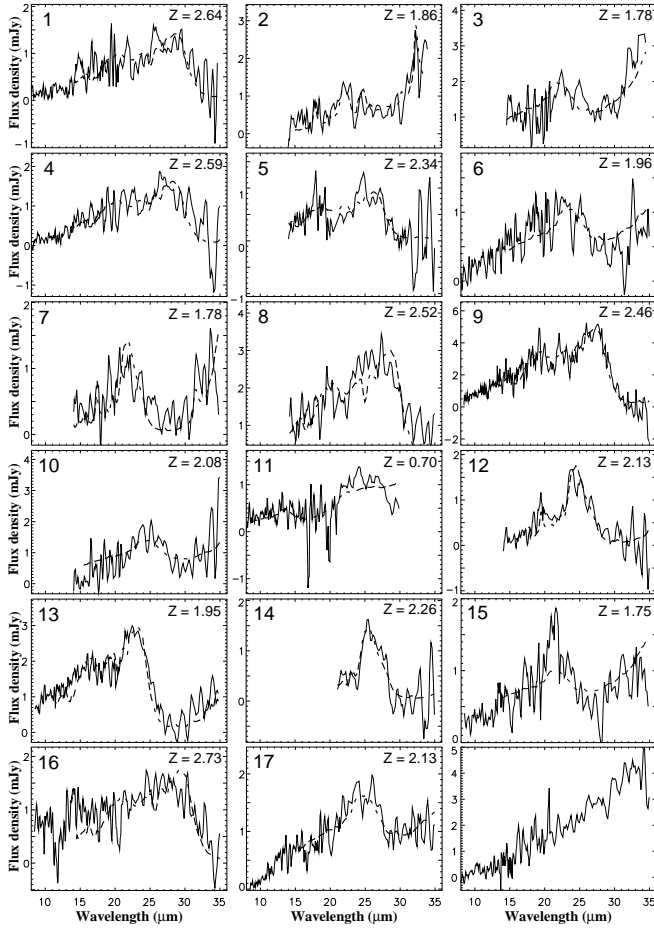


FIG. 1.— Observed spectra smoothed to approximate resolution of individual IRS orders (solid line), best template fit (dashed line), observed flux densities and redshift for all 17 sources in Table 1. Spectra truncated below $15 \mu\text{m}$ had no detectable signal in SL1; spectrum #14 also had no signal in LL2. Final panel is a source not listed in Table 1 to illustrate a spectrum without sufficient features for a redshift measurement.

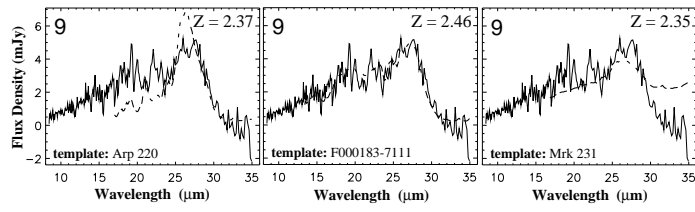


FIG. 2.— Spectra of source #9 showing alternative template fits with Arp220, absorbed ULIRG IRAS F000183-7111, and Mrk231. Range of z values illustrates uncertainty in z that arises from different template assumptions.